

Original article

# Assessment of CO<sub>2</sub>-energized fracturing methods: Their impacts on fracturing fluid flowback and CO<sub>2</sub> geological storage in deep tight gas reservoirs

Kaiqing Luo<sup>1,2</sup>, Hui Gao<sup>1,2\*</sup>, Yonggang Xie<sup>3,4</sup>, Zhanguo Ma<sup>4,5</sup>, Huazhou Li<sup>6</sup>, Zhilin Cheng<sup>1,2</sup>

<sup>1</sup>*School of Petroleum Engineering, Xi'an Shiyou University, Xi'an 710065, P. R. China*

<sup>2</sup>*Engineering Research Center of Development and Management for Low to Ultra-Low Permeability Oil & Gas Reservoirs in West China, Ministry of Education, Xi'an 710065, P. R. China*

<sup>3</sup>*Sulige South Operation Branch, PetroChina Changqing Oilfield Company, Xi'an 710018, P. R. China*

<sup>4</sup>*National Engineering Laboratory for Exploration and Development of Low-Permeability Oil & Gas Fields, Xi'an 710018, P. R. China*

<sup>5</sup>*Oil and Gas Technology Institute of Changqing Oilfield Company, PetroChina, Xi'an 710018, P. R. China*

<sup>6</sup>*School of Mining and Petroleum Engineering, Faculty of Engineering, University of Alberta, Edmonton T6G 1H9, Canada*

## Keywords:

CO<sub>2</sub>-energized fracturing  
fracturing fluid flowback  
CO<sub>2</sub> storage  
pore-scale fluid retention  
tight gas reservoirs

## Cited as:

Luo, K., Gao, H., Xie, Y., Ma, Z., Li, H., Cheng, Z. Assessment of CO<sub>2</sub>-energized fracturing methods: Their impacts on fracturing fluid flowback and CO<sub>2</sub> geological storage in deep tight gas reservoirs. *Advances in Geo-Energy Research*, 2026, 19(1): 58-71.

<https://doi.org/10.46690/ager.2026.01.05>

## Abstract:

CO<sub>2</sub>-energized fracturing holds great potential for enhancing fracturing fluid flowback and enabling effective CO<sub>2</sub> sequestration, while the effect of the choice of CO<sub>2</sub> energization strategy on these processes is not yet fully understood. This study experimentally investigated three representative CO<sub>2</sub> energization methods: Pre-fracturing injection, foam injection, and co-injection. Nuclear magnetic resonance techniques were applied to systematically analyze the influence of various CO<sub>2</sub> injection parameters on fracturing fluid flowback behavior and CO<sub>2</sub> storage in tight formations. The results showed that CO<sub>2</sub> pre-fracturing increases displacement pressure and significantly improves flowback efficiency, with optimal performance achieved at a moderate injection volume. Reducing the injection rate and increasing the volume further enhanced the CO<sub>2</sub> storage ratio. Foam injection facilitated flowback by improving foam quality, particularly in macropores. Co-injection achieved a favorable balance between high flowback efficiency and substantial CO<sub>2</sub> retention. Furthermore, the three energization strategies were shown to lead to distinct fluid redistribution patterns within porous media: Pre-fracturing promoted CO<sub>2</sub> retention in micropores and mesopores, foam injection reduced retention in macropores, and co-injection provided the most balanced performance in mesopores. These findings provide new insights into CO<sub>2</sub>-energized fracturing and sequestration mechanisms and offer technical guidance for optimizing CO<sub>2</sub>-based stimulation strategies in deep unconventional tight gas reservoirs.

## 1. Introduction

Natural gas continues to play a strategic role in modern energy systems due to its relatively low carbon intensity. Meanwhile, its sustained development increasingly depends

on the effective exploitation of tight and shale gas reservoirs (Gajanan et al., 2024; Kasala et al., 2024). As hydraulic fracturing remains the dominant stimulation technology, concerns regarding its water consumption, the resulting formation damage, and environmental impacts have motivated the search

for alternative approaches that simultaneously enhance recovery and reduce operational footprint (Middleton et al., 2015; Edwards et al., 2017; Osselin et al., 2019).

Among the emerging solutions, CO<sub>2</sub>-based fracturing has attracted growing attention because it not only mitigates some limitations of water-based fracturing but also provides opportunities for geological CO<sub>2</sub> storage (Iddphonce et al., 2020; Prasad et al., 2023; Zhou et al., 2025). Under deep reservoir conditions, CO<sub>2</sub> exhibits liquid-like density, gas-like viscosity and very low interfacial tension, enabling efficient penetration into micro- and nanopore systems and reducing capillary resistance (Kim et al., 2017). These properties of CO<sub>2</sub> enable a range of CO<sub>2</sub>-fracturing strategies, including pre-fracturing injection, co-injection with fracturing fluid, and foam-based systems that utilize higher viscosity and stability to improve proppant transport and fluid management (Qiao et al., 2024; Radhakrishnan et al., 2024; Harshini et al., 2025). Field trials across multiple basins worldwide have demonstrated the potential of these approaches to enhance fracture conductivity, improve reservoir connectivity, and promote both the solubility and mineral trapping of injected CO<sub>2</sub> (Zhou et al., 2019; Shen et al., 2024; Zhao et al., 2026).

Recent research has converged toward a mechanistic understanding of how CO<sub>2</sub> enhances stimulation performance (Agarwal and Kudapa, 2022; Cong et al., 2022; Chen et al., 2025). Studies of fracture propagation and CO<sub>2</sub>-rock interactions show that the strong gas-expansion energy of CO<sub>2</sub> plays a central role in driving fluid mobilization. Flowback behavior is strongly governed by permeability and pore-network connectivity, while the timing and spatial placement of injected CO<sub>2</sub> influence the distribution of gas within fractures and thus the effectiveness of liquid displacement (Li et al., 2021; Xia et al., 2022). Meanwhile, advances in CO<sub>2</sub> foam technologies highlight the importance of foam stability: More persistent foam structures can simultaneously improve flowback efficiency and increase CO<sub>2</sub> retention (Han et al., 2026). Numerical modeling further indicates that CO<sub>2</sub>-induced fracture complexity, phase behavior, and mineral-scale dissolution or extraction processes interact to enhance both hydrocarbon recovery and long-term CO<sub>2</sub> immobilization (Yeeken et al., 2018; Tao et al., 2025).

Despite the above advances, comparative analyses of different CO<sub>2</sub> energization methods, particularly with respect to fracturing fluid flowback and CO<sub>2</sub> storage in various pore structures, remain limited. Moreover, the solubility, miscibility and mobility of CO<sub>2</sub> further complicate flowback performance, and reservoir heterogeneities lead to inconsistent CO<sub>2</sub>-enhanced recovery and sequestration outcomes.

To address these research gaps and optimize CO<sub>2</sub>-energized fracturing under different energization modes, this study conducted three controlled laboratory experiments using cores from the Shanxi Formation in the Ordos Basin. This work compares CO<sub>2</sub> pre-fracturing, CO<sub>2</sub> foam and CO<sub>2</sub> co-injection, assessing their effects on fracturing fluid recovery and CO<sub>2</sub> storage. Through employing nuclear magnetic resonance (NMR) techniques to quantitatively analyze pore-scale fluid distribution and retention, the findings offer theoretical support for optimizing CO<sub>2</sub>-based fracturing and technologies

in deep unconventional tight gas reservoirs.

## 2. Materials and methods

### 2.1 Description and preparation of specimens

The tight sandstone samples used in this study were collected from the Shan 1 member of the Shanxi Formation in the Qingshui Gas Field, Ordos Basin (Fig. 1). This area features deep gas reservoirs, with the Shan 1 member typically buried at depths greater than 3,800 m and exhibiting an average reserve abundance of  $0.58 \times 10^8 \text{ m}^3/\text{km}^2$ . The reservoir is characterized by low porosity, low permeability, low abundance, and low pressure, along with a homogeneous gas-bearing sequence, small sand-body scale, and thin gas layers (Fu et al., 2019).

Samples were collected from depths ranging from 4,427.48 to 4,482.24 m, and the cores primarily consisted of gray medium-grained sandstone. The statistical analysis of 74 cores showed an average porosity of 5.37% and an average permeability of 0.1967 mD. Overall mineralogical analysis indicated that the tight sandstones were uniformly quartz-rich, with quartz typically accounting for 76.5%-79.1%, accompanied by moderate clay minerals (approximately 12.1%-14.5%) and minor feldspar (about 5.1%-7.3%), while other minerals remained below 4%. For this experiment, simulated formation water representing the gas reservoir was prepared with a salinity of 20.94 g/L and a CaCl<sub>2</sub> water type. Pure (99.99%) CO<sub>2</sub> gas was used, and the fracturing fluids comprised a guar gum-based system and a foam fracturing fluid supplied by the oilfield.

### 2.2 Experimental apparatus and procedures

#### 2.2.1 Experimental apparatus

This study included three types of CO<sub>2</sub> energization experiments: CO<sub>2</sub> pre-fracturing energization, CO<sub>2</sub> foam energization, and CO<sub>2</sub> co-injection energization. As illustrated in Fig. 2, the experimental setup comprised a core holder equipped with a corrosion-resistant rubber sleeve, a syringe pump (accuracy  $\leq \pm 1\%$ , flow rate range of 0.01 to 10 mL/min), a hand pump, a high-temperature and high-pressure intermediate container, a wet gas flow meter (accuracy  $\pm 1\%$  of full-scale reading, measurement range of 0 to 30 L/min), and an electronic balance. To characterize pore-scale fluid distribution and flowback behavior, a Niumag PQ001 NMR instrument was used to obtain the *T*<sub>2</sub> spectra of the fracturing fluid before and after flowback. The key acquisition parameters were set as follows: An echo time of 0.1 ms; a wait time of 2,500 ms; and 5,000 echoes were accumulated for each scan to ensure a high signal-to-noise ratio.

#### 2.2.2 Experimental scheme and procedure

To simulate the effects of various CO<sub>2</sub> injection methods on energization and flowback, three experimental groups were designed according to typical CO<sub>2</sub>-energized fracturing operations. For CO<sub>2</sub> pre-fracturing, the injection volume was set within the range of 0.3-0.7 pore volumes (PV) to ensure adequate pressurization while avoiding premature gas

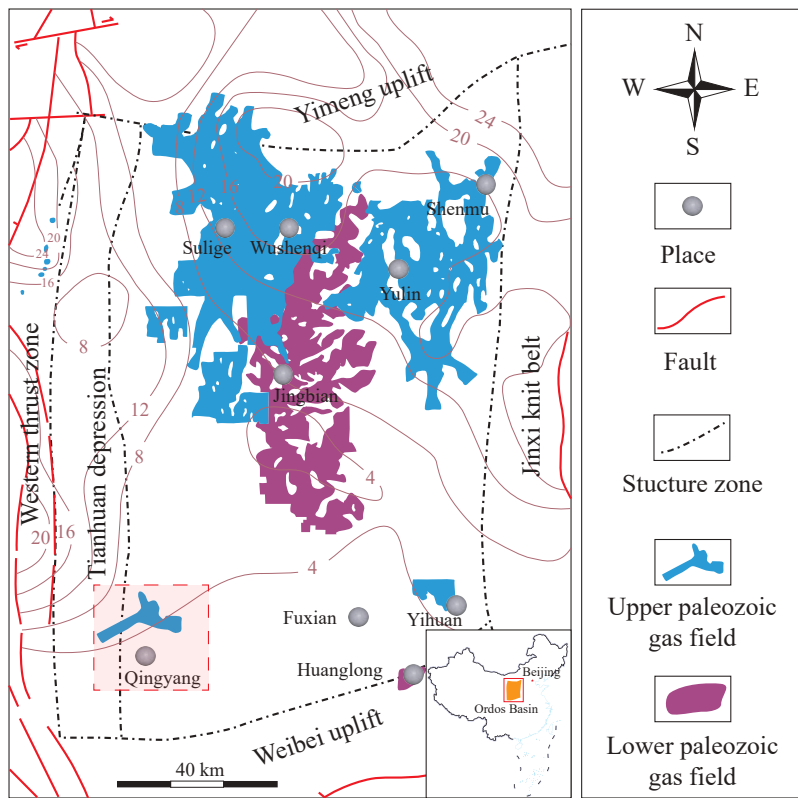


**Fig. 1.** Geographical location of the collected specimens, modified from Fu et al. (2019) and Zou et al. (2024).

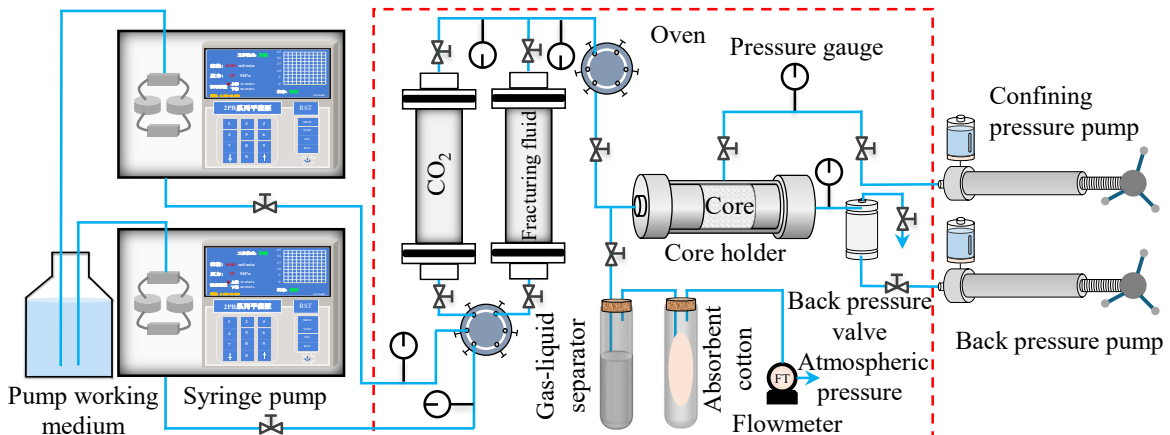


**Fig. 2.** Experimental device for  $\text{CO}_2$ -energized fracturing fluid flowback and storage.

breakthrough. For  $\text{CO}_2$  foam energization, foam qualities of 55%-75% were set, as this range has been shown to balance foam stability while achieving an effective displacement of fracturing fluid (Zhao et al., 2024). Similarly, for  $\text{CO}_2$  co-injection, a co-injection ratio of 25%-40% was selected based on evidence that this range enhances the combined benefits of  $\text{CO}_2$ -induced energy and fracturing fluid displacement while avoiding operational challenges associated with higher  $\text{CO}_2$  fractions (Wang et al., 2019).

These experiments aimed to evaluate the impacts of  $\text{CO}_2$  pre-fracturing energization,  $\text{CO}_2$  foam energization, and  $\text{CO}_2$  co-injection energization. The experiments were conducted

under varying conditions, including injection volumes and rates, foam qualities, and co-injection ratios, to systematically evaluate the  $\text{CO}_2$ -enhanced flowback effects and storage patterns. The experimental temperature and initial injection pressure were set at 80 °C and 15 MPa, respectively. The detailed experimental parameters are provided in Tables 1-3. A comprehensive overview of the experimental workflow is illustrated in Fig. 3. The diagram shows the process of  $\text{CO}_2$ -energized fracturing fluid flowback and  $\text{CO}_2$  storage, outlining the key stages involved, from initial  $\text{CO}_2$  injection and pressure stabilization to the flowback of fracturing fluid and the subsequent evaluation of  $\text{CO}_2$  storage.

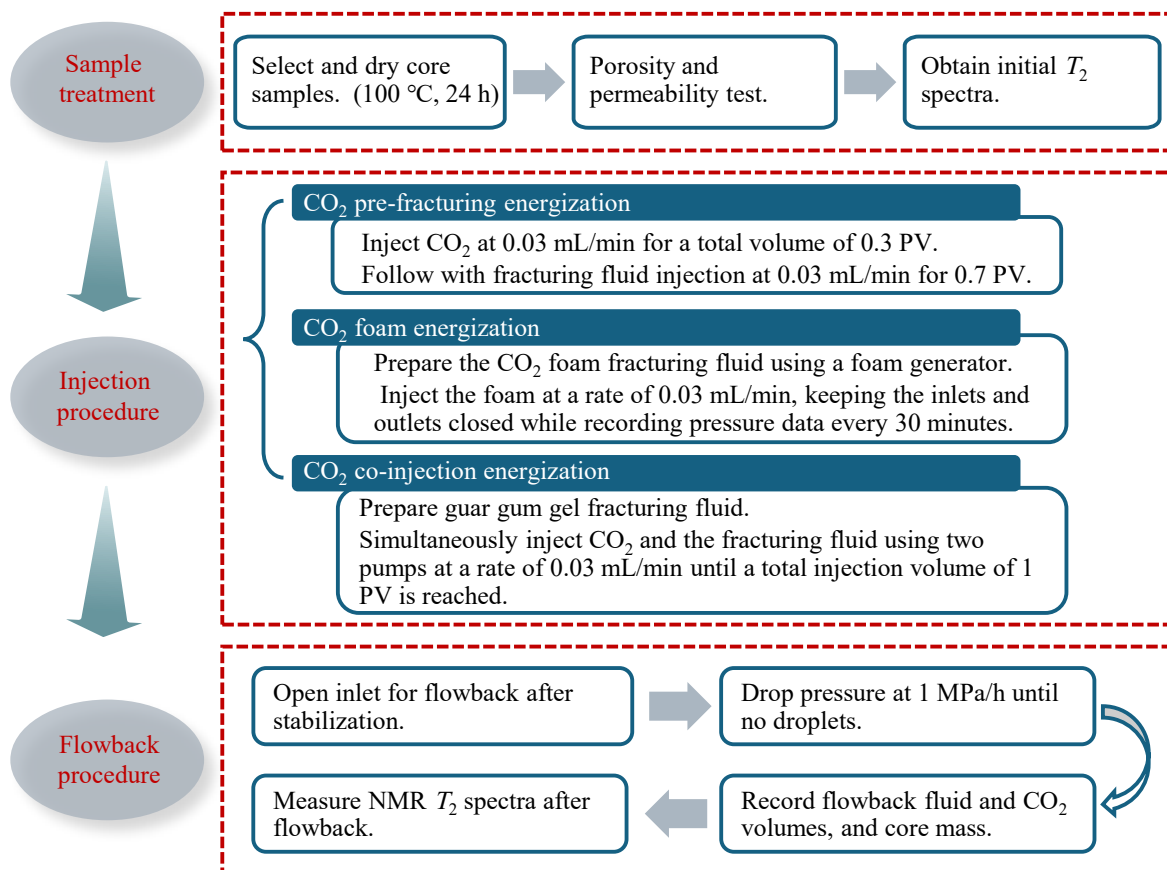


**Fig. 3.** Flowchart of CO<sub>2</sub>-energized fracturing fluid flowback and storage processes.

**Table 1.** Core properties and injection parameters for CO<sub>2</sub> pre-fracturing energization.

| No. | Porosity (%) | Permeability (mD) | Injection speed (mL/min) | CO <sub>2</sub> injection volume (PV) |
|-----|--------------|-------------------|--------------------------|---------------------------------------|
| P-1 | 5.16         | 0.1242            | 0.03                     | 0.3                                   |
| P-2 | 4.96         | 0.1052            | 0.03                     | 0.5                                   |
| P-3 | 4.59         | 0.1153            | 0.03                     | 0.7                                   |
| P-4 | 4.66         | 0.1341            | 0.06                     | 0.5                                   |
| P-5 | 7.54         | 0.1258            | 0.09                     | 0.5                                   |

### 2.3 Pore structure classification

The NMR  $T_2$  spectrum provides an effective characterization of tight sandstone pore structures, where  $T_2$  is positively correlated with pore size, while signal amplitude reflects pore volume and spectrum continuity indicates pore connectivity (Eynlal et al., 2023; Gao et al., 2023a; Luo et al., 2026). Using conventional cutoffs of 10 and 100 ms (Wang et al., 2020), pores are classified into micropores (0-10 ms), mesopores (10-100 ms) and macropores (100-10,000 ms). As shown in Fig. 4, the samples exhibit bimodal to trimodal spectra dominated by micropore signals, with mesopores moderately developed and macropores being the least abundant, aligning with the

**Table 2.** Core properties and injection parameters for CO<sub>2</sub> foam energization.

| No. | Porosity (%) | Permeability (mD) | Injection speed (mL/min) | Foam quality (%) |
|-----|--------------|-------------------|--------------------------|------------------|
| F-1 | 6.58         | 0.1543            | 0.03                     | 55               |
| F-2 | 6.55         | 0.1249            | 0.03                     | 65               |
| F-3 | 5.34         | 0.1351            | 0.03                     | 75               |

typical pore-structure characteristics of tight sandstone (Gao et al., 2025). Based on the representative spectra (P-1, C-1, and C-1-fb), the integrated  $T_2$  areas before and after flowback ( $A_0$  and  $A_1$ ) were used to quantitatively assess the changes in retained fluid.

### 2.4 Fracturing fluid flowback and CO<sub>2</sub> storage evaluation method

To eliminate the impact of CO<sub>2</sub> on the measured volume of fracturing fluid, the flowback rate was calculated using the gravimetric method:

$$R_1 = \frac{m_2}{m_1 + m_2 - m_0} \times 100\% \quad (1)$$

where  $R_1$  represents the flowback rate of the fracturing fluid, %;  $m_0$  denotes the dry weight of the core, g;  $m_1$  denotes the

**Table 3.** Core properties and injection parameters for CO<sub>2</sub> co-injection energization.

| No. | Porosity (%) | Permeability (mD) | Injection speed (mL/min) | Co-injection ratio (%) |
|-----|--------------|-------------------|--------------------------|------------------------|
| C-1 | 4.53         | 0.1166            | 0.03                     | 25                     |
| C-2 | 3.52         | 0.1353            | 0.03                     | 33                     |
| C-3 | 4.06         | 0.1452            | 0.03                     | 40                     |

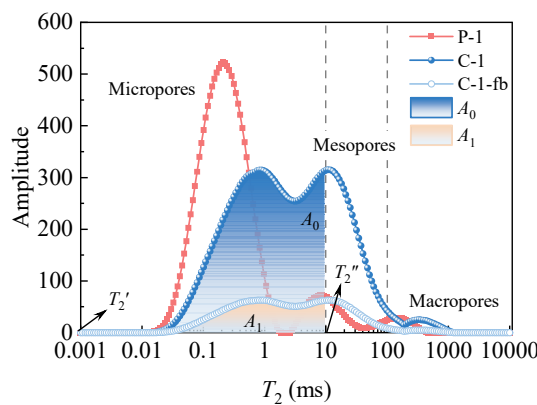


**Fig. 4.** Diagram illustrating the pore-structure classification of typical tight sandstone samples.

wet weight of the core after flowback, g; and  $m_2$  is the mass of the flowback fluid, g.

A gas flow meter was used to measure CO<sub>2</sub> flowback, and the CO<sub>2</sub> volume was corrected to the reservoir conditions using the gas state equation to calculate the CO<sub>2</sub> storage ratio:

$$R_2 = \frac{V_0 - V_1}{V_0} \times 100\% \quad (2)$$

where  $R_2$  represents the CO<sub>2</sub> storage ratio, %;  $V_0$  denotes the injected volume of CO<sub>2</sub>, mL; and  $V_1$  is the volume of CO<sub>2</sub> produced during flowback, mL.

To quantitatively characterize the retention patterns of fracturing fluid in the core under different CO<sub>2</sub> energization methods, NMR technology was used to assess the distribution of fracturing fluid across various pore scales. The retention rate of the fracturing fluid in the core was calculated by determining the ratio of the  $T_2$  spectral area within each pore-size interval before and after flowback:

$$R_3 = \frac{\sum_{T_2'}^{T_2''} A_1}{\sum_{T_2'}^{T_2''} A_0} \times 100\% \quad (3)$$

where  $R_3$  represents the retention rate of the fracturing fluid in the core, %;  $A_1$  denotes the signal amplitude within a specific pore size range of the NMR  $T_2$  spectrum after flowback, and  $A_0$  is the signal amplitude corresponding to the initial NMR  $T_2$  spectrum of the core in the same pore size range.

It should be noted that potential sources of uncertainty in the calculated flowback rate, CO<sub>2</sub> storage ratio, and fluid retention include gas flow meter errors, volume measurement

deviations, pressure and temperature fluctuations, and the heterogeneity of core permeability. To minimize these effects, all instruments were calibrated before each test, and the experimental procedures were performed under standardized and controlled conditions.

### 3. Experimental results

#### 3.1 Pressure variation in the core displacement system

The pressure response of the displacement system clearly differentiates the energization effectiveness of the three CO<sub>2</sub> injection strategies (Fig. 5). CO<sub>2</sub> pre-fracturing generates the strongest pressure enhancement, rising sharply with slug volume and peaking at 0.5 PV (Fig. 5(a)), beyond which further pore filling leads to a plateau, while higher injection rates accelerate the early pressure rise but yield similar stabilized pressures of 26.54 MPa (Fig. 5(b)).

CO<sub>2</sub> foam energization also generates substantial pressure buildup, and the effect strengthens systematically with foam quality. Pressure increments rise from 10.61 to 12.15 MPa as foam quality increases from 55% to 75%, producing final system pressures of 25.61 to 27.15 MPa (Fig. 5(c)). However, once the foam quality approaches the upper stability limit, the pressure enhancement begins to level off due to reduced foam robustness.

In contrast, CO<sub>2</sub> co-injection yields the weakest energization, with the maximum pressure increase reaching only 7.92 MPa at a 40% co-injection ratio and a final pressure of 22.92 MPa (Fig. 5(d)). Although increasing the CO<sub>2</sub> co-injection ratio elevates pressure through gas expansion, the limited CO<sub>2</sub> fraction and early onset of gas-liquid phase separation constrain the maximum pressure increase, which remains significantly lower than that of pre-fracturing or foam energization.

Overall, the pressure evolution trends indicate that pre-fracturing and CO<sub>2</sub> foam mobilize fluids primarily through compressible-energy storage and stabilized gas-phase displacement, whereas co-injection provides only partial energization due to restricted gas volume and reduced sweep continuity.

#### 3.2 Variation in the fracturing fluid flowback rate and CO<sub>2</sub> storage ratio

The flowback behavior and CO<sub>2</sub> storage patterns further distinguish the three energization strategies (Fig. 6). In CO<sub>2</sub> pre-fracturing, increasing the initial CO<sub>2</sub> volume enhances fracturing fluid flowback, peaking at 79.55% around 0.5 PV, while CO<sub>2</sub> storage gradually increases due to effective pore filling and compression (Fig. 6(a)). Higher injection speed accelerates early fluid displacement but reduces overall CO<sub>2</sub> retention, as rapid flow limits dissolution and capillary trapping (Fig. 6(b)). With rising foam quality (77.27%-89.36%), CO<sub>2</sub> foam energization progressively improves flowback while maintaining relatively stable CO<sub>2</sub> storage (36.56%-39.11%), reflecting the combined effects of gas expansion and reduced liquid-phase resistance (Fig. 6(c)). In contrast, CO<sub>2</sub> co-injection yields moderate flowback, with most CO<sub>2</sub> dissolving

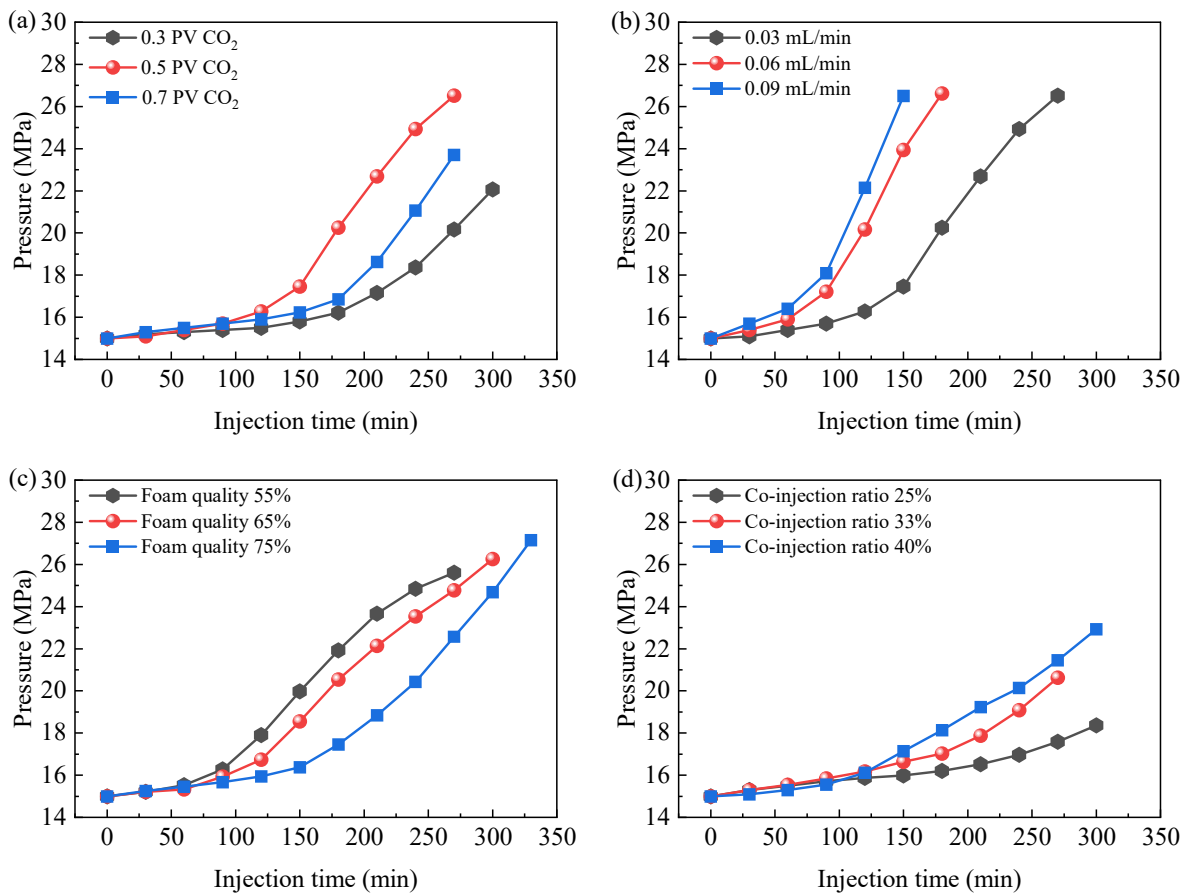


**Fig. 5.** Pressure evolution in the core displacement system under different  $\text{CO}_2$  energization conditions: (a)  $\text{CO}_2$  injection volume, (b)  $\text{CO}_2$  injection rate, (c) foam quality and (d)  $\text{CO}_2$  co-injection ratio.

into the fracturing fluid and returning simultaneously, resulting in relatively low storage efficiency (average 37.62%, Fig. 6(d)).

The higher  $\text{CO}_2$  storage observed at lower injection rates is attributed to prolonged  $\text{CO}_2$  residence and enhanced interaction with the pore network. Slower injections allow  $\text{CO}_2$  to dissolve more thoroughly into formation water under stable pressure, reducing premature gas-phase breakout. Reduced viscous forces enable  $\text{CO}_2$  to penetrate smaller pores and become immobilized via capillary trapping. Extended contact time further promotes interactions with clay minerals, facilitating partial carbonation and long-term mineral sequestration (Gao et al., 2023b).

### 3.3 Microscopic retention patterns of fracturing fluid

After the flowback of the fracturing fluid, retention patterns were analyzed using NMR testing methods. Figs. 7-9 display several peaks in the  $T_2$  spectrum: The micropore peak has the highest amplitude, followed by the mesopore peak, and the macropore peak shows the lowest amplitude. After flowback, the signal amplitude for micropores remains the highest across different energization methods, while mesopores and macropores exhibit relatively low amplitudes.

Figs. 7(a)-7(e) illustrate the  $T_2$  spectra for fracturing fluid

retention under the  $\text{CO}_2$  pre-fracturing energization method. At an injection volume of 0.5 PV, the retention rates for different pore sizes are relatively low, with those of micropores, mesopores and macropores at 26.82%, 11.29%, and 11.81%, respectively. Increasing the injection speed leads to decreased retention rates across all pore sizes. At an injection speed of 0.09 mL/min, retention rates reach their lowest levels, with micropores, mesopores and macropores retention rates of 15.07%, 16.60% and 17.01%, respectively. The  $T_2$  spectra exhibit a dominant micropore peak (0-10 ms) both before and after flowback. At 0.5 PV injection, the signal amplitude for micropores decreases by 26.82%, while mesopores (10-100 ms) and macropores (>100 ms) show reductions of 11.29% and 11.81%, respectively. This indicates that  $\text{CO}_2$  preferentially displaces the fracturing fluid from larger pores due to its low viscosity and high diffusivity. However, capillary forces in micropores resist  $\text{CO}_2$  penetration, leading to higher fluid retention in these micropores.

Under the  $\text{CO}_2$  foam energization method, the flowback of fracturing fluid from macropores is highly efficient, resulting in a retention rate of 0% (Fig. 8(a)-8(c)). At foam qualities of 55%, 65% and 75%, the retention rates in micropores are relatively high at 28.92%, 22.33% and 12.34%, respectively, while the retention rates in mesopores are lower at 17.41%,

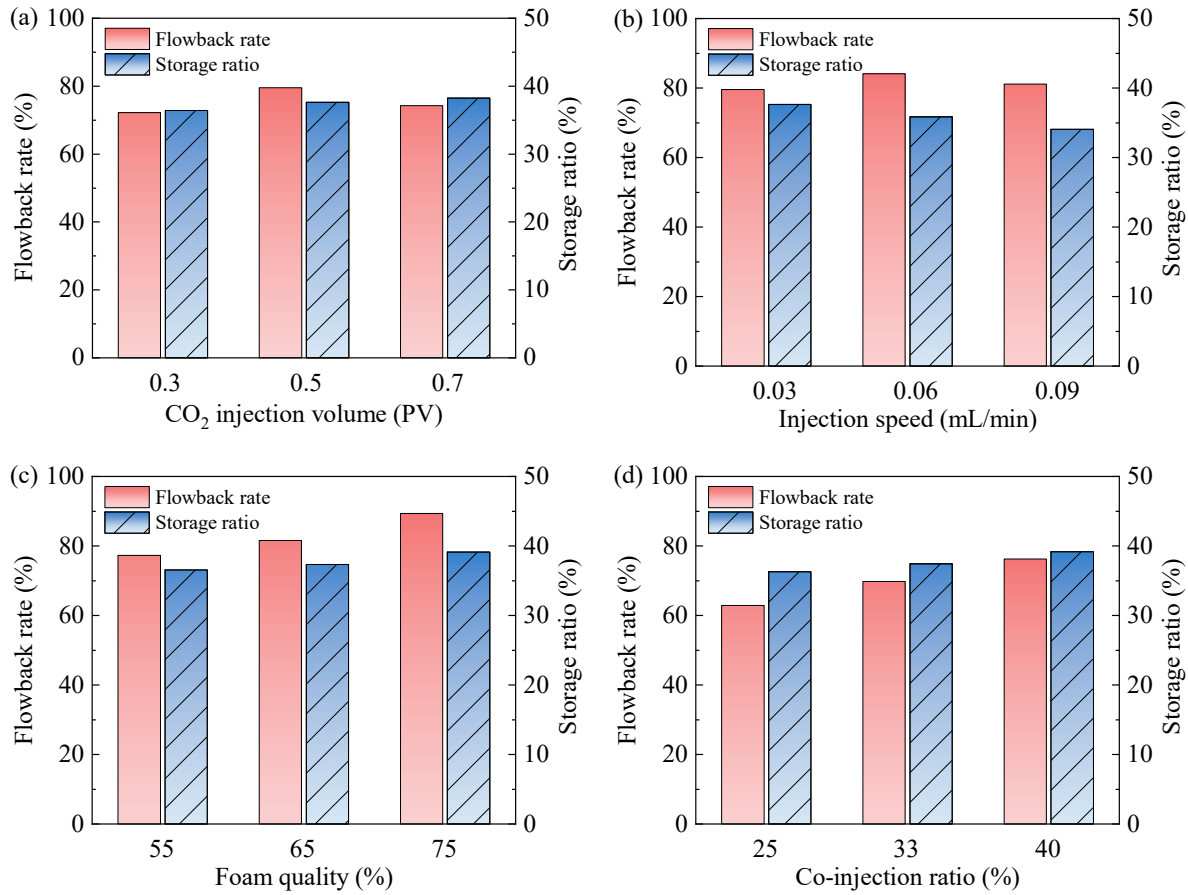


**Fig. 6.** Variation in fracturing fluid flowback rate and CO<sub>2</sub> storage ratio under different CO<sub>2</sub> energization conditions: (a) CO<sub>2</sub> injection volume, (b) CO<sub>2</sub> injection rate, (c) foam quality, and (d) CO<sub>2</sub> co-injection ratio.

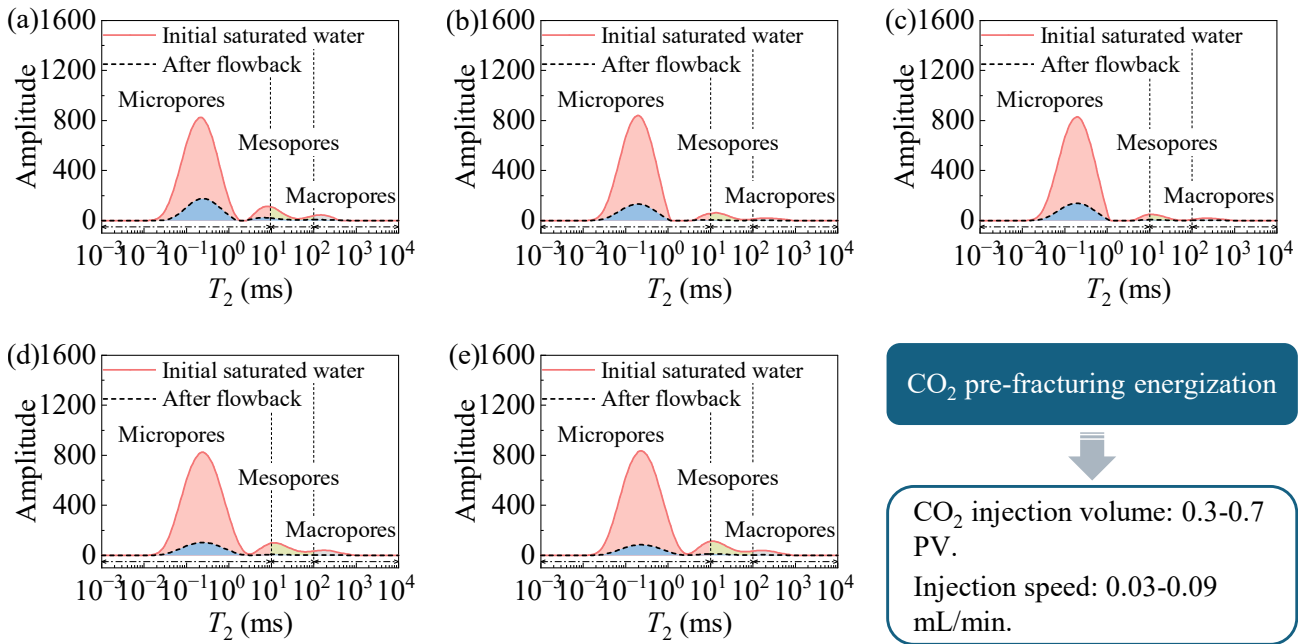


**Fig. 7.** Microscopic retention characteristics of fracturing fluid under CO<sub>2</sub> pre-fracturing energization with varying injection parameters: (a)-(c) CO<sub>2</sub> injection volumes of 0.3, 0.5 and 0.7 PV, and (d)-(e) CO<sub>2</sub> injection speeds of 0.06 and 0.09 mL/min.

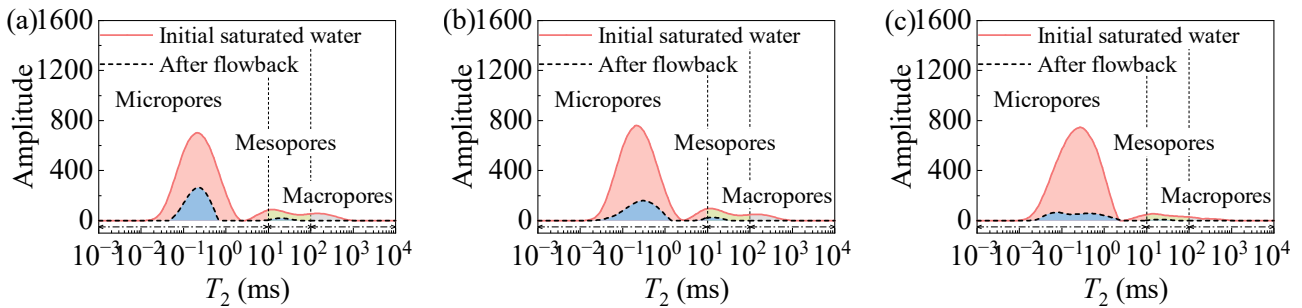


**Fig. 8.** Microscopic retention characteristics of fracturing fluid under  $\text{CO}_2$  foam energization with varying foam quality: (a) 55%, (b) 65% and (c) 75%.

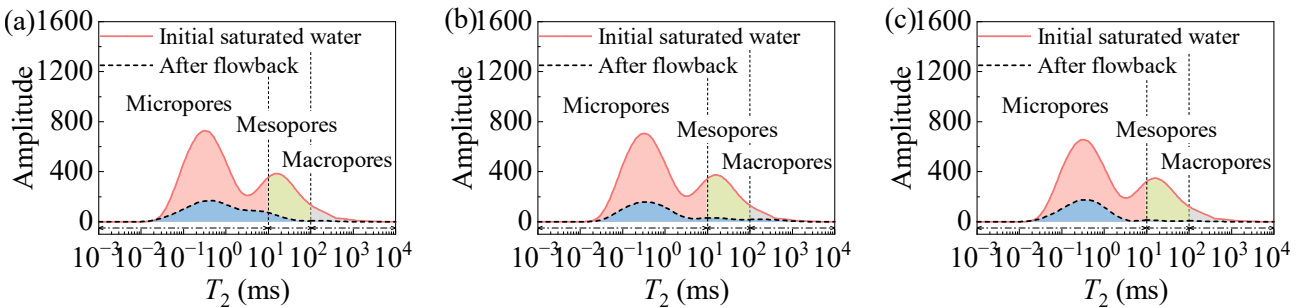


**Fig. 9.** Microscopic retention characteristics of fracturing fluid under  $\text{CO}_2$  co-injection energization with varying  $\text{CO}_2$  ratio: (a) 25%, (b) 33% and (c) 40%.

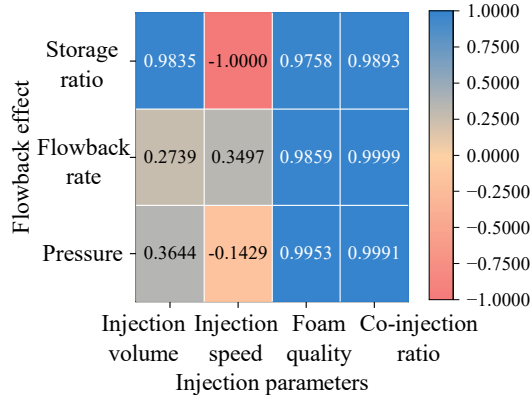


**Fig. 10.** Correlation analysis of the key factors influencing  $\text{CO}_2$  energization and enhanced flowback.

17.84% and 13.01%. The  $T_2$  spectra show near-complete elimination of the macropore peak ( $> 100$  ms) after flowback. For instance, at 75% foam quality, macropore retention drops to 0%, while micropore retention decreases to 12.34%. This can be attributed to the foam lamellae bridging macropore throats, reducing fluid mobility and promoting efficient flowback. The bimodal  $T_2$  distribution post-flowback reflects the stability of foam in larger pores, while residual fracturing fluid remains trapped in smaller pores due to high capillary resistance.

In contrast, the  $\text{CO}_2$  co-injection energization method shows higher overall retention rates in micropores after flowback (Fig. 9(a)-9(c)). For co-injection ratios of 25%, 33% and 40%, the retention rates in micropores are 50.66%, 41.64% and

34.10%, respectively. The average retention rate in macropores across different co-injection ratios is 22.16%, while the retention rate in mesopores is the lowest, averaging 11.31%. The  $T_2$  spectra show a marked reduction in mesopore retention, with the trimodal distribution shifting to a dominant micro-pore peak post-flowback. This indicates that co-injected  $\text{CO}_2$  preferentially displaces fluid from mesopores. However, the continued retention in micropores underscores the difficulty of mobilizing fluids within ultra-tight pore networks.

## 4. Discussion

### 4.1 Influencing factors of $\text{CO}_2$ energization and flowback effects

To analyze the effects of various  $\text{CO}_2$  energization methods, a Pearson correlation analysis was conducted to quantitatively assess the influence of experimental parameters on core displacement system pressure, fracturing fluid flowback rate, and  $\text{CO}_2$  storage ratio. The correlation coefficient  $r$  was calculated to quantify the degree of correlation, as given by:

$$r_{xy} = \frac{\sum_{i=1}^n (x_i - \bar{x})(y_i - \bar{y})}{\sqrt{\sum_{i=1}^n (x_i - \bar{x})^2 \cdot \sum_{i=1}^n (y_i - \bar{y})^2}} \quad (4)$$

where  $r_{xy}$  represents the Pearson correlation coefficient between variables  $x$  and  $y$ ,  $n$  represents the number of observations,  $x_i$  and  $y_i$  denote the individual sample points indexed with  $i$ , and  $\bar{x}$  and  $\bar{y}$  denote the sample means of variables  $x$

and  $y$ , respectively.

Typically, a coefficient  $r \geq 0.8$  indicates a strong correlation,  $0.5 \leq r < 0.8$  signifies a moderate correlation, and  $r < 0.5$  reflects a weak correlation (An et al., 2022). The results of the correlation analysis are presented as a correlation heatmap in Fig. 10.

The correlation coefficient results reveal significant differences in the effects of various  $\text{CO}_2$  energization methods on displacement system pressure, fracturing fluid flowback rate and  $\text{CO}_2$  storage ratio. For  $\text{CO}_2$  pre-fracturing energization, the amount of injected  $\text{CO}_2$  shows a low correlation with system pressure and fracturing fluid flowback rate but a high correlation with the  $\text{CO}_2$  storage ratio. This indicates that variations in  $\text{CO}_2$  injection volume have minimal impact on system pressure and fracturing fluid flowback, especially regarding the influence of increased injection volume. In the experiments, the narrow  $\text{CO}_2$  injection range and the low porosity of tight sandstone characterized by abundant micropores allow the rock matrix to buffer pressure increases. Furthermore, the high compressibility of supercritical  $\text{CO}_2$  and its partial dissolution in the fracturing fluid leads to complex gas-liquid interactions, resulting in minimal pressure changes despite the increased  $\text{CO}_2$  injection rate.

The injection speed shows a high negative correlation with the  $\text{CO}_2$  storage ratio, with minimal effects on fracturing fluid flowback and displacement system pressure. A higher injection speed hinders pressure diffusion, weakening the  $\text{CO}_2$  energization effect. With less time for  $\text{CO}_2$  to dissolve into the fracturing fluid and interact with the reservoir rock,  $\text{CO}_2$  retention in the reservoir decreases.

In the  $\text{CO}_2$  foam energization mode, a strong positive correlation with displacement system pressure, fracturing fluid flowback rate and  $\text{CO}_2$  storage ratio can be observed. This indicates that increasing the  $\text{CO}_2$  foam quality effectively enhances the energization effects as more  $\text{CO}_2$  dissolves in the fracturing fluid. During depressurization and flowback, the dissolved supercritical  $\text{CO}_2$  escapes, reducing resistance to fluid flow and enhancing liquid production. As foam quality increases, the gas phase becomes more dominant and the foam becomes less viscous, which improves the mobility of the fracturing fluid. This is especially true for macropores, where  $\text{CO}_2$  displacement is more efficient.

In the  $\text{CO}_2$  co-injection energization mode, the high compressibility of  $\text{CO}_2$  compared to the fracturing fluid indicates that increasing the co-injection ratio can improve both  $\text{CO}_2$  storage and fracturing fluid flowback rates. Higher  $\text{CO}_2$  ratios increase the amount of injected  $\text{CO}_2$ , enhancing the energy available for fluid displacement.

In summary,  $\text{CO}_2$  pre-fracturing energization has a relatively weak effect on displacement system pressure and fracturing fluid flowback, whereas foam energization and co-injection energization methods significantly impact fracturing fluid flowback, core displacement system pressure and  $\text{CO}_2$  storage. Increasing foam quality and co-injection ratios can enhance fracturing fluid flowback rates and improve  $\text{CO}_2$  storage efficiency. Overall, optimizing the foam fracturing fluid system benefits  $\text{CO}_2$  energization effects. A significant negative relationship exists between injection speed and  $\text{CO}_2$

storage ratio, which can be attributed to the fact that higher injection speeds reduce the residence time of  $\text{CO}_2$  in the reservoir. With less time for  $\text{CO}_2$  to dissolve into the fracturing fluid and interact with the reservoir rock,  $\text{CO}_2$  retention in the reservoir decreases. Additionally, faster injection speeds may bypass smaller pore spaces, where  $\text{CO}_2$  dissolution and retention are the most effective, thus leading to reduced  $\text{CO}_2$  storage efficiency.

The energization and flowback outcomes are clearly illustrated by the quantitative assessment of various  $\text{CO}_2$  energization methods on core displacement system pressure, fracturing fluid flowback rate and  $\text{CO}_2$  storage ratio. As shown in Fig. 11, displacement system pressure is positively correlated with  $\text{CO}_2$  injection volume, foam quality and  $\text{CO}_2$  co-injection ratio, but it is negatively correlated with  $\text{CO}_2$  injection speed. Notably,  $\text{CO}_2$  pre-fracturing energization has the weakest impact on displacement system pressure, while foam and co-injection methods exert a more substantial influence. This suggests that, given a constant injection volume, increasing the proportion of injected  $\text{CO}_2$  enhances reservoir pressure. The efficiency of fracturing fluid flowback is significantly influenced by various injection parameters, with a positive correlation between different energization methods and fracturing fluid flowback rates. This indicates that  $\text{CO}_2$  energization effectively improves the fracturing fluid flowback rate, which can be enhanced by further optimizing the  $\text{CO}_2$  injection parameters.

The  $\text{CO}_2$  storage ratio is highly sensitive to the injection parameters: It increases with  $\text{CO}_2$  injection volume, foam quality, and co-injection ratio, while it decreases with injection speed. This quantitative correlation is consistent with our experimental observations. For instance, as shown in Section 3.2, reducing the  $\text{CO}_2$  injection speed from 0.09 to 0.03 mL/min raises the average storage ratio from 34.07% to 37.63%. These results confirm that adopting lower injection rates is an effective strategy to enhance  $\text{CO}_2$  storage efficiency in tight sandstones.

#### 4.2 Distribution of fracturing fluid before and after flowback

The flowback patterns of fracturing fluid under  $\text{CO}_2$  pre-fracturing energization method were quantitatively characterized by NMR testing at different stages. Fig. 12 presents the distribution of pore fluid in the core at different scales before and after fracturing fluid flowback. The pie charts, indicated by the blue arrows, illustrate the post-flowback distribution of fracturing fluid in the pores under each experimental condition. The proportion of pore fluid in micropores increases after flowback, while that in mesopores and macropores decreases. During flowback, as displacement system pressure declines,  $\text{CO}_2$  in the pores expands, preferentially displacing fluid from macropores and mesopores, which leads to a greater volume of fracturing fluid being retained in micropores. This phenomenon aligns with the findings of Zhou et al. (2023), who reported that in tight sandstone,  $\text{CO}_2$  preferentially displaces fluids from larger pores, while capillary forces lead to higher retention in micropores.

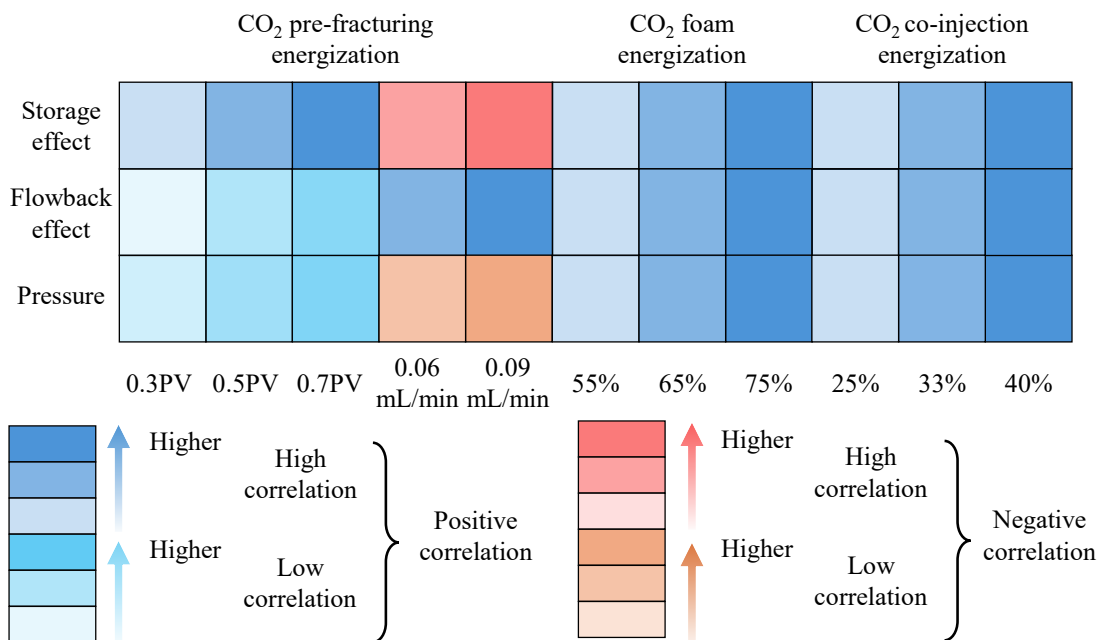


**Fig. 11.** Correlation analysis of energization effects under different  $\text{CO}_2$  injection parameters.

For the F1-F3 cores,  $\text{CO}_2$  foam energization facilitates flowback, increasing fluid proportions in both micropores and mesopores after flowback, while the proportion in macropores decreases (Fig. 13). The average proportions of pore fluid in micropores before and after flowback are 90.92% and 94.92%, respectively. The presence of  $\text{CO}_2$  foam reduces the seepage resistance in the pores, enhancing efficient flowback from macropores. Zheng et al. (2023) suggested that the  $\text{CO}_2$  foam effect alters pore size and connectivity, impacting fluid distribution and flowback efficiency. This aligns with our findings, which show that  $\text{CO}_2$  foam-enhanced recovery improves fluid flowback by modifying pore structure and reducing seepage resistance.

In the C1-C3 cores using  $\text{CO}_2$  co-injection for energization, the proportion of pore fluid in micropores increases after flowback, while a decrease is observed in mesopores; changes in macropores are more complex (Fig. 14). Under  $\text{CO}_2$  co-injection conditions, flowback from mesopores is particularly effective, with proportions before and after flowback at 22.75% and 7.26%, respectively. Co-injecting energizing foam with a quality of less than 52% significantly increases the return speed and rate of the fracturing fluid, reduces its retention, and mitigates water blocking damage, thereby improving stimulation effectiveness.

#### 4.3 Mechanisms of $\text{CO}_2$ energization and geological storage

During the  $\text{CO}_2$  energization and flowback process, injected  $\text{CO}_2$  serves two main functions: It dissolves in the fracturing fluid, thus reducing flow resistance, and expands during flowback, facilitating efficient fluid return. Fig. 15 illustrates how  $\text{CO}_2$  is utilized in fracturing operations through capture and transport. After the injection phase, the well is closed for a certain period, allowing interactions among the injected

$\text{CO}_2$ , fracturing fluid and reservoir. This interaction enhances reservoir properties, such as effective permeability and pore connectivity, by reducing mineral blockage and increasing porosity. It also modifies wettability and lowers capillary forces, promoting more efficient flowback of the fracturing fluid. When the well reopens,  $\text{CO}_2$  aids in effective flowback, with some  $\text{CO}_2$  retained in the reservoir for geological storage. A portion of  $\text{CO}_2$  is permanently stored underground through physical and chemical mechanisms. In physical terms,  $\text{CO}_2$  is trapped in reservoir pore spaces by capillary forces and dissolved in formation water. Chemically,  $\text{CO}_2$  reacts with minerals like calcite to form stable carbonate compounds, a process known as mineral trapping (Prasad et al., 2023). This mineral sequestration converts  $\text{CO}_2$  into a solid, enhancing the effective permeability and stability of the reservoir.

The effects of different  $\text{CO}_2$  energization methods vary significantly, influenced by injection parameters affecting displacement system pressure, flowback rate and  $\text{CO}_2$  storage efficiency. In  $\text{CO}_2$  pre-fracturing, the initial  $\text{CO}_2$  slug, due to its low viscosity and high mobility, invades larger pores and fractures in the rock. During the subsequent injection of fracturing fluid, this pre-positioned  $\text{CO}_2$  is compressed, storing significant elastic energy. The NMR results indicate that the highest residual fracturing fluid saturation is found in micropores, suggesting that the compressed  $\text{CO}_2$  preferentially expands and displaces fluid from macropores and mesopores upon pressure release. However, due to strong capillary forces, it remains trapped in the micropores, leaving them water-saturated.

The foam energization method improves the efficiency of fluid injection, enhances flowback rates and minimizes damage to reservoir permeability and fracture conductivity. The NMR data reveals a remarkable, near-complete clearance of fracturing fluid from macropores after flowback, especially

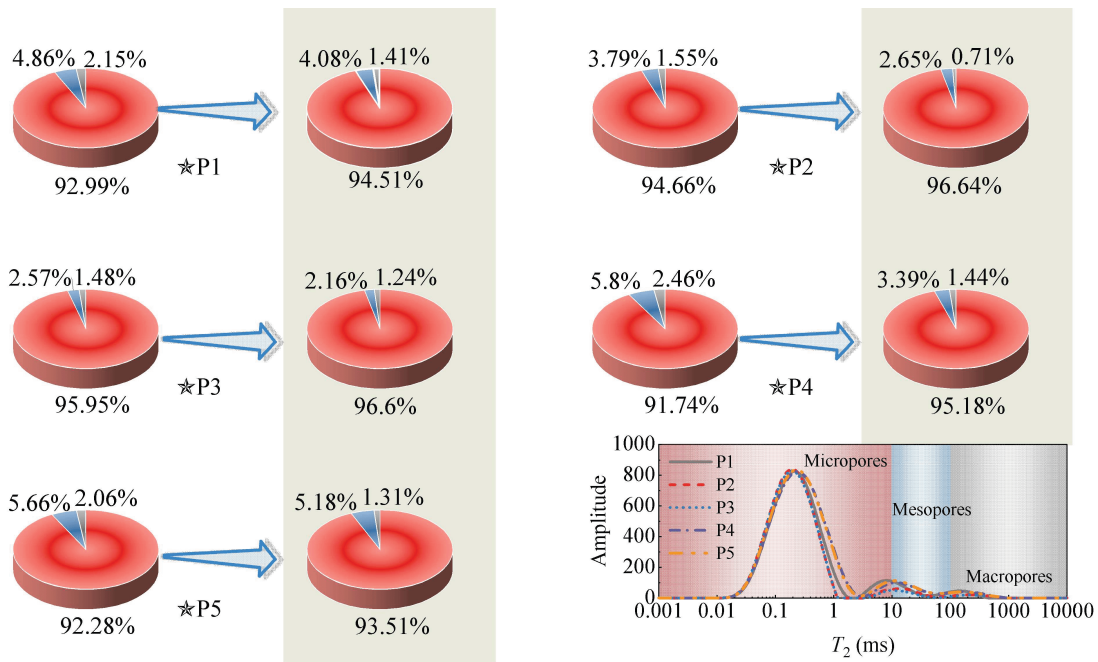


**Fig. 12.** Variation in fracturing fluid distribution before and after flowback under the  $\text{CO}_2$  pre-fracturing energization method.

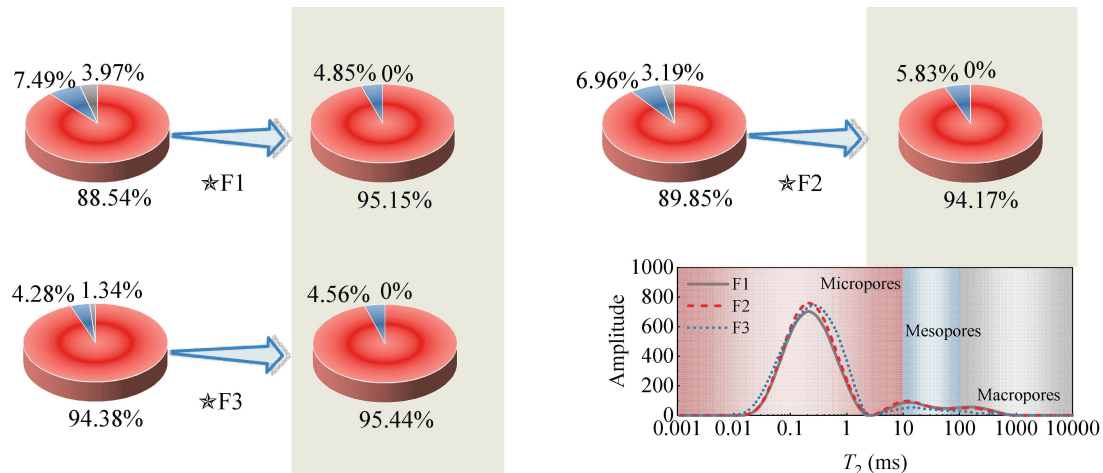


**Fig. 13.** Variation in fracturing fluid distribution before and after flowback under the  $\text{CO}_2$  foam energization method.

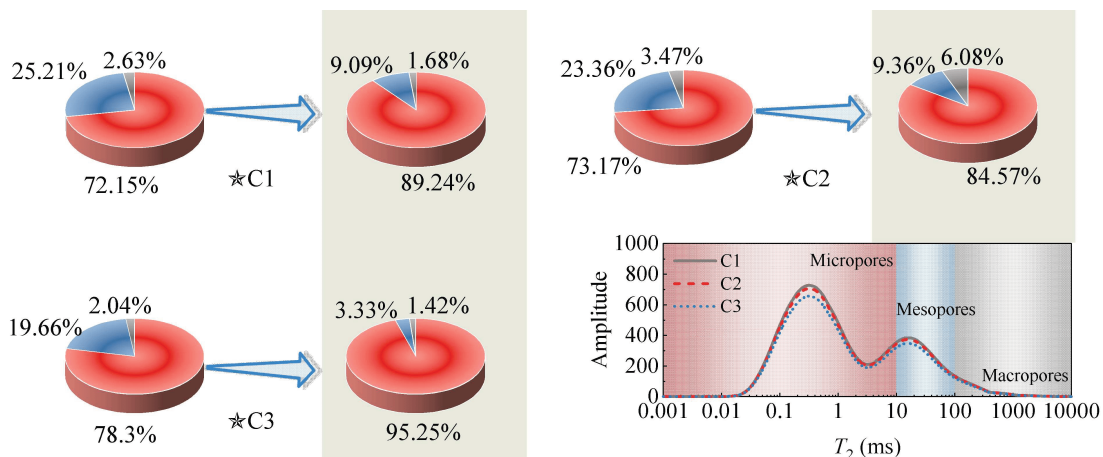


**Fig. 14.** Variation in fracturing fluid distribution before and after flowback under the  $\text{CO}_2$  co-injection energization method.

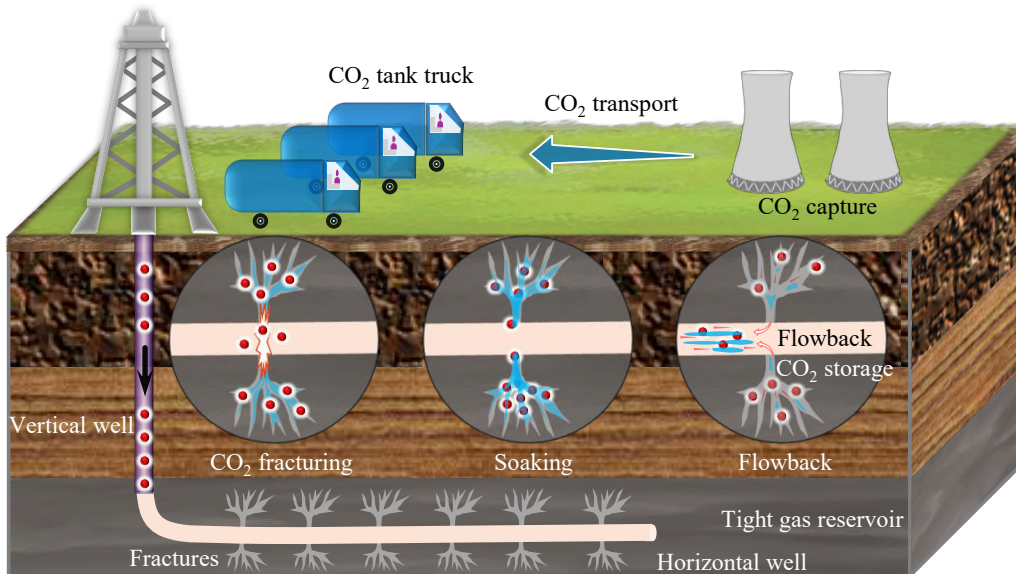


**Fig. 15.** Schematic representation of mechanisms for CO<sub>2</sub> fracturing and geological storage.

at high foam quality. This occurs because the lamellae of the foam effectively block the throats of large pores, preventing gas channeling and forcing the displacing front to efficiently displace resident fluid. Additionally, the expansion of CO<sub>2</sub> generates energy that enhances the flowback capacity of the fluid. During flowback, the release of elastic energy from the gas due to pressure drop rapidly lifts the fluid to the surface, allowing compressed foam bubbles to expand and exit through the wellbore.

CO<sub>2</sub> co-injection energization simplifies fluid injection, promoting the dissolution of CO<sub>2</sub> in the fluid. The NMR results demonstrate that this method is uniquely effective at displacing fluid from mesopores, showing the lowest average retention rate in this range. This suggests that the co-injected CO<sub>2</sub> can access and mobilize fluid from these intermediate-sized pores more effectively than the other methods. The expansion of heated CO<sub>2</sub> in the formation increases reservoir energy, while CO<sub>2</sub> also reduces the surface tension of the fluid, enhancing both flowback speed and rate.

In summary, injected CO<sub>2</sub> dissolves in the fluid, easing injection difficulty and improving energization effectiveness. The reaction of supercritical CO<sub>2</sub> with water can dissolve specific minerals in the core, enhancing transport properties and injectivity. During flowback, dissolved supercritical CO<sub>2</sub> causes volume expansion, increasing pressure and facilitating the rapid flowback of fluid. The properties of supercritical CO<sub>2</sub>, such as low viscosity, high diffusion coefficient and extremely low surface tension, contribute to increased flowback energy and reduced seepage and capillary resistance. Overall, injected CO<sub>2</sub> plays a crucial role in expanding fractures, improving reservoir properties and enhancing the flowback of fluid. During fracturing, well soaking and flowback, a substantial amount of CO<sub>2</sub> is consumed through the synergistic effects of adsorption, dissolution and expansion, facilitating geological storage.

#### 4.4 Application of CO<sub>2</sub>-energized fracturing methods in oilfields

Supercritical CO<sub>2</sub>, given its low viscosity, high diffusivity and near-zero surface tension, efficiently penetrates micro-fractures and promotes fracture-network development, making CO<sub>2</sub> fracturing well suited for low-permeability and water-sensitive reservoirs. Furthermore, it reduces water use and enables partial CO<sub>2</sub> sequestration during injection and flowback.

Field applications across multiple basins consistently show accelerated fluid cleanup and enhanced early production when CO<sub>2</sub> is introduced as an energizing agent (Wang et al., 2014; Abdel et al., 2024; Tang et al., 2025). Pre-fracturing CO<sub>2</sub> slugs expand rapidly during flowback, improving fluid return and stimulated reservoir volume, while CO<sub>2</sub> foam systems couple energization with superior fluid and proppant transport to deliver substantial production gains.

Our experimental results align with these observations, showing that CO<sub>2</sub> foam and pre-fracturing outperform co-injection due to stronger pressure buildup and more effective gas expansion. Each energization mode displays pore-structure-dependent advantages: CO<sub>2</sub> pre-fracturing enhances mobilization in micropores, CO<sub>2</sub> foam performs best in macropores, and CO<sub>2</sub> co-injection suits mesoporous media. These insights support more targeted designs for CO<sub>2</sub>-energized fracturing and improved predictions of flowback and storage performance.

### 5. Conclusions

- 1) CO<sub>2</sub> pre-fracturing energization at an optimal injection volume of 0.5 PV significantly boosts fracturing efficiency and system pressure, primarily enhancing fluid flowback from micropores and mesopores. CO<sub>2</sub> foam energization, with a foam quality of 75%, facilitates near-complete fluid recovery in macropores. In contrast, CO<sub>2</sub> co-injection energization demonstrates superior efficiency

- in mesopores, achieving an average retention rate of 11.31%.
- 2) Lower injection rates improve the CO<sub>2</sub> storage ratio, aligning fracturing operations with carbon sequestration goals. The suitability of each energization method varies with pore structure: CO<sub>2</sub> pre-fracturing energization is ideal for tight sandstones with micropores, CO<sub>2</sub> foam energization benefits macropore-rich formations, and CO<sub>2</sub> co-injection energization is suited for mesopore-dominated reservoirs.
- 3) All three CO<sub>2</sub> energization methods enhance reservoir properties through mechanisms such as CO<sub>2</sub> dissolution, fluid expansion and chemical reactions. These processes promote effective geological CO<sub>2</sub> storage and improve flowback efficiency. Optimizing CO<sub>2</sub> energization strategies can significantly enhance both fracturing fluid flowback and CO<sub>2</sub> storage capacity, offering substantial benefits for the development of deep unconventional gas reservoirs.

## Acknowledgements

The authors acknowledge the financial support provided by the National Natural Science Foundation of China (Nos. 52174030 and 52474042), the Natural Science Basic Research Program of Shaanxi (No. 2025JC-JCQN-013), and the National Science and Technology Major Project of China (No. 2025ZD1404804).

## Conflicts of interest

The authors declare no competing interest.

**Open Access** This article is distributed under the terms and conditions of the Creative Commons Attribution (CC BY-NC-ND) license, which permits unrestricted use, distribution, and reproduction in any medium, provided the original work is properly cited.

## References

- Abdel, M., Al-Mefleh, S. K., Al-Muhanna, D., et al. Successful application of CO<sub>2</sub> foam fracturing enables paradigm shift in stimulation strategy of North Kuwait Jurassic depleted reservoirs. Paper IPTC 23591 Presented at International Petroleum Technology Conference, Dhahran, Saudi Arabia, 12-14 February, 2024.
- Agarwal, M., Kudapa, V. K. Comparing the performance of supercritical CO<sub>2</sub> fracking with high energy gas fracking in unconventional shale. *MRS Energy and Sustainability*, 2022, 9: 461-468.
- An, Q., Zhang, Q., Li, X., et al. Accounting for dynamic alteration effect of SC-CO<sub>2</sub> to assess role of pore structure on rock strength: A comparative study. *Energy*, 2022, 260: 125125.
- Chen, H., Wei, B., Zhou, X., et al. Theory and technology of enhanced oil recovery by gas and foam injection in complex reservoirs. *Advances in Geo-Energy Research*, 2025, 15(3): 181-184.
- Cong, Z., Li, Y., Pan, Y., et al. Study on CO<sub>2</sub> foam fracturing model and fracture propagation simulation. *Energy*, 2022, 238: 121778.
- Edwards, R. W., Doster, F., Celia, M. A., et al. Numerical modeling of gas and water flow in shale gas formations with a focus on the fate of hydraulic fracturing fluid. *Environmental Science & Technology*, 2017, 51(23): 13779-13787.
- Eyinla, D. S., Leggett, S., Badrouri, F., et al. A comprehensive review of the potential of rock properties alteration during CO<sub>2</sub> injection for EOR and storage. *Fuel*, 2023, 353: 129219.
- Fu, J., Wie, X., Luo, S., et al. Discovery and geological knowledge of the large deep coal-formed Qingyang Gas Field, Ordos Basin, NW China. *Petroleum Exploration and Development*, 2019, 46(6): 1111-1126.
- Gajanan, K., Ranjith, P., Yang, S., et al. Advances in research and developments on natural gas hydrate extraction with gas exchange. *Renewable and Sustainable Energy Reviews*, 2024, 190: 114045.
- Gao, H., Luo, K., Wang, C., et al. Impact of dissolution and precipitation on pore structure in CO<sub>2</sub> sequestration within tight sandstone reservoirs. *Petroleum Science*, 2025, 22(2): 868-883.
- Gao, H., Wang, C., Cheng, Z., et al. Effect of pressure pulse stimulation on imbibition displacement within a tight sandstone reservoir with local variations in porosity. *Geoenergy Science and Engineering*, 2023a, 226: 211811.
- Gao, H., Xie, Y., Cheng, Z., et al. A minireview of the influence of CO<sub>2</sub> injection on the pore structure of reservoir rocks: Advances and outlook. *Energy & Fuels*, 2023b, 37(1): 118-135.
- Han, B., Gao, H., Xiao, Y., et al. CO<sub>2</sub> foam-assisted fracturing fluid flowback and CO<sub>2</sub> sequestration in tight sandstone gas reservoirs: Experimental and numerical study. *Geoenergy Science and Engineering*, 2026, 257: 214199.
- Harshini, R., Ranjith, P. G., Kumari, W. G. P. CO<sub>2</sub> foam vs. conventional Methods: Enhancing deep geothermal energy recovery in extreme conditions. *Renewable Energy*, 2025, 256: 123905.
- Iddphonce, R., Wang, J., Zhao, L. Review of CO<sub>2</sub> injection techniques for enhanced shale gas recovery: Prospect and challenges. *Journal of Natural Gas Science and Engineering*, 2020, 77: 103240.
- Kasala, E. E., Wang, J., Lwazi, H. M., et al. The influence of hydraulic fracture and reservoir parameters on the storage of CO<sub>2</sub> and enhancing CH<sub>4</sub> recovery in yanchang formation. *Energy*, 2024, 296: 131184.
- Kim, T. H., Cho, J., Lee, K. S. Evaluation of CO<sub>2</sub> injection in shale gas reservoirs with multi-component transport and geomechanical effects. *Applied Energy*, 2017, 190: 1195-1206.
- Li, L., Chen, Z., Su, Y., et al. Experimental investigation on enhanced-oil-recovery mechanisms of using supercritical carbon dioxide as prefracturing energized fluid in tight oil reservoir. *SPE Journal*, 2021, 26(5): 3300-3315.
- Luo, K., Gao, H., Wang, X., et al. Mechanism of water blocking damage in tight sandstone gas reservoirs: Novel insights from differential spectrum analysis of 2D NMR data. *Measurement*, 2026, 258: 119360.

- Middleton, R. S., Carey, J. W., Currier, R. P., et al. Shale gas and non-aqueous fracturing fluids: Opportunities and challenges for supercritical CO<sub>2</sub>. *Applied Energy*, 2015, 147: 500-509.
- Osselin, F., Saad, S., Nightingale, M., et al. Geochemical and sulfate isotopic evolution of flowback and produced waters reveals water-rock interactions following hydraulic fracturing of a tight hydrocarbon reservoir. *Science of the Total Environment*, 2019, 687: 1389-1400.
- Prasad, S. K., Sangwai, J. S., Byun, H.-S. A review of the supercritical CO<sub>2</sub> fluid applications for improved oil and gas production and associated carbon storage. *Journal of CO<sub>2</sub> Utilization*, 2023, 72: 102479.
- Qiao, M., Jing, Z., Zhou, R., et al. The throttling characteristics of supercritical carbon dioxide in the flowback process of CO<sub>2</sub> fracturing. *Gas Science and Engineering*, 2024, 121: 205184.
- Radhakrishnan, A., Chang, B., DiCarlo, D., et al. CO<sub>2</sub> foam rheology in rough shale and sandstone fractures at elevated temperatures. *Fuel*, 2024, 366: 131373.
- Shen, W., Ma, T., Zuo, L., et al. Advances and prospects of supercritical CO<sub>2</sub> for shale gas extraction and geological sequestration in gas shale reservoirs. *Energy & Fuels*, 2024, 38(2): 789-805.
- Tang, W., Zhou, F., Sheng, J. J., et al. Further investigation of CO<sub>2</sub> energization fracturing in shale reservoir—from microscopic mechanism to field application. *Fuel*, 2025, 385: 134156.
- Tao, Z., Wu, Y., Liu, X., et al. The synergistic mechanism of CO<sub>2</sub> fracturing stimulation and storage of tight oil reservoirs using a cohesive zone model. *Physics of Fluids*, 2025, 37(8): 086631.
- Wang, F., Cao, P., Wang, Y., et al. Combined effects of cyclic load and temperature fluctuation on the mechanical behavior of porous sandstones. *Engineering Geology*, 2020, 266: 105466.
- Wang, H., Li, X., Sepehrnoori, K., et al. Calculation of the wellbore temperature and pressure distribution during supercritical CO<sub>2</sub> fracturing flowback process. *International Journal of Heat and Mass Transfer*, 2019, 139: 10-16.
- Wang, X., Wu, J., Zhang, J. Application of CO<sub>2</sub> fracturing technology for terrestrial shale gas reservoirs. *Natural Gas Industry*, 2014, 34(1): 64-67. (in Chinese)
- Xia, Y., Li, L., Wang, Z. Experimental and numerical study on influencing factors of replacement capacity and slick-water flowback efficiency using pre-CO<sub>2</sub> fracturing in tight oil reservoirs. *Journal of Petroleum Science and Engineering*, 2022, 215: 110697.
- Yekeen, N., Padmanabhan, E., Idris, A. K. A review of recent advances in foam-based fracturing fluid application in unconventional reservoirs. *Journal of Industrial and Engineering Chemistry*, 2018, 66: 45-71.
- Zhao, D., Liu, Y., Ma, Z., et al. CO<sub>2</sub> adaptive functional materials: Perspectives in geological utilization and sequestration. *Advances in Colloid and Interface Science*, 2026, 348: 103718.
- Zhao, J., Wu, T., Pu, W., et al. Application status and research progress of CO<sub>2</sub> fracturing fluid in petroleum engineering: A brief review. *Petroleum*, 2024, 10(1): 1-10.
- Zheng, Y., Zhai, C., Chen, A., et al. Microstructure evolution of bituminous coal modified by high-pressure CO<sub>2</sub> foam fracturing fluid with different treatment times. *Natural Resources Research*, 2023, 32(3): 1319-1338.
- Zhou, H., Yan, T., Trivedi, J., et al. Investigating rock properties and fracture propagation pattern during supercritical CO<sub>2</sub> pre-fracturing in conglomerate reservoir. *Advances in Geo-Energy Research*, 2025, 17(2): 95-106.
- Zhou, J., Hu, N., Xian, X., et al. Supercritical CO<sub>2</sub> fracking for enhanced shale gas recovery and CO<sub>2</sub> sequestration: Results, status and future challenges. *Advances in Geo-Energy Research*, 2019, 3(2): 207-224.
- Zhou, X., Li, L., Sun, Y., et al. Investigation of influence factors on CO<sub>2</sub> flowback characteristics and optimization of flowback parameters during CO<sub>2</sub> dry fracturing in tight gas reservoirs. *Petroleum Science*, 2023, 20(6): 3553-3566.
- Zou, C., Li, Y., He, X., et al. Contrasting hydrocarbon reservoirs in the North China Craton in relation to inhomogeneous craton destruction. *Earth-Science Reviews*, 2024, 255: 104843.